

# **PREDICTING BEHAVIOR OF AP-1000 NUCLEAR REACTOR FUEL ROD UNDER STEADY STATE OPERATING CONDITION BY USING FRAPCON-4.0 SOFTWARE**

*NGUYEN VAN TUNG, NGUYEN THANH THUY, CAO DUY MINH, NGUYEN TRONG HUNG*  
*Institute for technology of radioactive and rare elements*  
*Email: tungnn.88@gmail.com*

## **ABSTRACT**

This paper reports the results on the predictions of behavior of AP-1000 nuclear reactor fuel rod under steady state operating condition by using FRAPCON-4.0 software. The predictive items were the temperature distribution in the fuel rod, including fuel centerline temperature, fuel pellet surface temperature, gas temperature, cladding inside and outside temperature, oxide surface and bulk coolant temperature; and gap conductance and thickness. The predictive data were suggested the fuel rod thermal behavior image in nuclear reactor. The predictive items also include deformation of fuel pellets, fission gas release and rod internal pressure, cladding oxidation and hydration.

## **I. INTRODUCTION**

Uranium dioxide (UO<sub>2</sub>) fuel ceramic is the main material used in most types of existing nuclear power plant. Nuclear fuel for heavy water reactors are manufactured from natural uranium. For light water reactors, U<sup>235</sup> fuel must be enriched 3-5% [1-2]. Evaluating state of UO<sub>2</sub> pellets in particular and nuclear fuel in general in the nuclear reactor is very important to establish the safety criteria of nuclear fuel. The quality of the UO<sub>2</sub> pellets is assessed on the safety standards of each nation or organization. Under steady-state operating condition, the evaluations are assessed by software's such as FRAPCON, TRANURANUS, COSMOS, FEMAXI, FUELROD and etc. FRAPCON-4.0 code, one of fuel performance codes verified and licensed by United States Nuclear Regulatory Commission (NRC) to review fuel design of Light Water Reactor (LWR), is designed to perform the thermal-mechanical calculations of LWR fuel rod such as the temperature, pressure, and deformation as functions of time-dependent fuel rod power and coolant boundary conditions [3-5]. FRAPCON-4.0 code uses data of material properties documented in the updated version of the MATPRO material properties package for high burn-up conditions and advanced cladding alloy such as Zircaloy-2, Zircaloy-4, ZIRLO™, M5 and etc. [5]. The main models of FRAPCON-4.0 code used in the calculations include the FRACAS-I thermal-mechanical model and Forsberg-Massih fission gas release model. In the study and our previous [6], the latest version of the steady state fuel performance code,

FRAPCON-4.0, was utilized to predict the thermal behavior of fuel rod under steady-state operating condition in reactor. And fuel rod design of AP-1000 designed by Westinghouse Electric Corporation was input data for the code [6-7]. FRAPCON-4.0 software was supported by Vietnam Atomic Energy Agency.

## II. CALCULATION MODEL FOR AP-1000 FUEL ROD

### Description of AP-1000 fuel rod design

The AP-1000 fuel rods consist of cylindrical, ceramic pellets of slightly enriched uranium dioxide ( $UO_2$ ). These pellets are contained in cold-worked and stress-relieved ZIRLO tubing, which is plugged and seal-welded at the ends to encapsulate the fuel. ZIRLO is an advanced zirconium-based alloy. The  $UO_2$  pellets are slightly dished to better accommodate thermal expansion and fuel swelling, and to increase the void volume for fission product release. The void volume will also accommodate the differential thermal expansion between the clad and the fuel as the pellet density increases in response to irradiation. An AP-1000 fuel rod comprises the following parts: Upper plug, cladding, lower plug, fuel pellets and a spring [7-9].

### Modeling method

The AP-1000 fuel rod has been modeled using FRAPCON-4.0 code based on the design parameters, reference data in the operation of AP-1000 reactor [7-9]. The dimensions for AP-1000 fuel rod were taken from design data. The fuel rod was divided into 24, 17, 45 and 9 number of time steps, (fuel) radial boundaries, (equal-volume) radial rings and (equal-length) axial nodes, respectively [4, 10]. The axial and radial nodes are numbered from bottom to top of total active fuel height and from the fuel rod centerline to the cladding outside surface, respectively. Main parameters of the boundary conditions were given in Table 1. Calculations were performed for 3 fuel cycles; the length of each cycle was 351 effective full power days.

**Table 1.** Main parameters of the boundary conditions

<b>Parameter</b>	<b>Value</b>
The rod initial fill pressure, in Mpa	2.35
Coolant system pressure, in Mpa	15.5
Coolant inlet temperature, in K	552.6
Mass flux of coolant, in $kg/(s.m^2)$	3466
Linear heat generation rate, in kW/m	
1 <sup>st</sup> cycle	18.4
2 <sup>nd</sup> cycle	20.3
3 <sup>rd</sup> cycle	20.2

The temperature distribution throughout the fuel and coolant was calculated at each axial node. A schematic of the temperature distribution at an arbitrary axial node might be found in the document [4].

### III. RESULTS AND DISCUSSIONS

#### 3.1. Predicted fuel rod temperature distribution predictions as a function of burnup

Table 2 is summaries of predicting the fuel rod temperature distribution calculated by FRAPCON-4.0 code. Fig.1. show image thermal behavior of fuel rod.

**Table 2.** Results of the thermal calculations

Axial node		Temperature, in K					
		$T_{fc}$	$T_{fs}$	$T_{ci}$	$T_{co}$	$T_{ox}$	$T_b$
Node 1	Maximum	1098.4	775.2	595.1	577.7	576.7	562.7
	Nominal	1058.9	727.7	593.8	576.7	576.3	562.6
Node 2	Maximum	1345.4	851.2	618.5	592.0	588.7	567.1
	Nominal	1322.6	738.4	615.4	589.4	587.9	567.0
Node 3	Maximum	1400.4	861.8	627.7	600.1	595.1	572.6
	Nominal	1362.8	731.3	624.0	596.6	594.4	572.3
Node 4	Maximum	1393.7	863.9	634.0	606.6	600.3	578.0
	Nominal	1358.8	732.8	629.3	602.2	599.4	577.6
Node 5	Maximum	1383.1	863.7	639.0	612.6	604.9	583.3
	Nominal	1342.9	735.0	633.7	607.4	603.9	582.8
Node 6	Maximum	1363.4	863.5	644.6	618.8	609.4	588.3
	Nominal	1328.2	737.5	638.0	612.4	608.1	587.7
Node 7	Maximum	1357.7	866.3	650.3	625.0	613.8	593.1
	Nominal	1324.0	738.3	642.7	617.5	612.5	592.4
Node 8	Maximum	1309.8	856.9	651.8	628.6	616.5	597.6
	Nominal	1278.9	747.1	643.9	620.6	615.2	596.7
Node 9	Maximum	1107.5	799.1	637.3	620.9	614.2	601.0
	Nominal	1067.3	743.3	631.5	615.5	612.6	600.1
Rod fuel nominal	Maximum	1306.6	766.7	633.1	609.1	602.2	582.6
	Nominal	1271.6	736.8	628.0	604.3	601.1	582.1

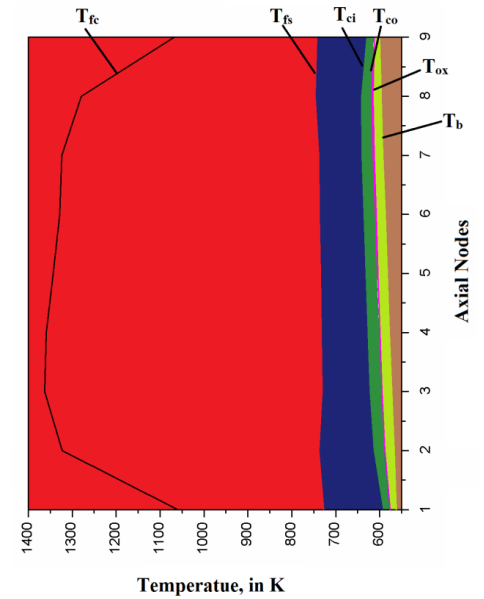


**Fig. 1.** Image thermal behavior of fuel rod.

The predictive data show that the centerline temperature ( $T_{fc}$ ) reaches its maximum of 1400.4 K and was lower than the limit value of the AP-1000 nuclear reactor fuel rod design  $T_{fc}(\text{max.}) = 2866.3$  K (for prevention of centerline melt) [7]. The maximum of average fuel centerline temperature was 1306.6K. The fuel centerline temperature at the bottom (node 9) and top (node 1) of the fuel rod was lower than that at the center (from node 2 to node 8) of the fuel rod. The reason is that the distribution of neutron flux in the core of the reactor varies depending

on the operation and control of the reactor. Also for this reason, the deformation of fuel pellets along the fuel rods axis also varies according to the location of the fuel pellets.

The temperature difference between the fuel centerline and fuel pellet surface temperature ( $\Delta T$ ) was predicted. The maximum temperature difference is 711K at node 3 and node 4, but at the top and end of the fuel column, the temperature difference is lower, about 385 K, for 4.1 mm of radius of pellets. The reason is also the distribution of neutron flux in the core of the reactor varies depending on the operation and control of the reactor. And at each node positions, temperature difference increases with the operating time. Thus, the thermal conductivity of the fuel pellets increases with operating time.

The heat transfer from the fuel surface to the cladding inside depends on the thermal conductivity of the gap. Fig. 2 shows the predicted thermal conductivity and the change thickness of the gap. Thus, gap conductance was very high; its maximum calculated by the code was approximate 90 kW/(m<sup>2</sup>.K) and the fuel clad gap was closure due to cladding creep down and the fuel pellet solid fission product swelling; the gap thickness calculated by the code was 2.6  $\mu\text{m}$  during 3 cycles.

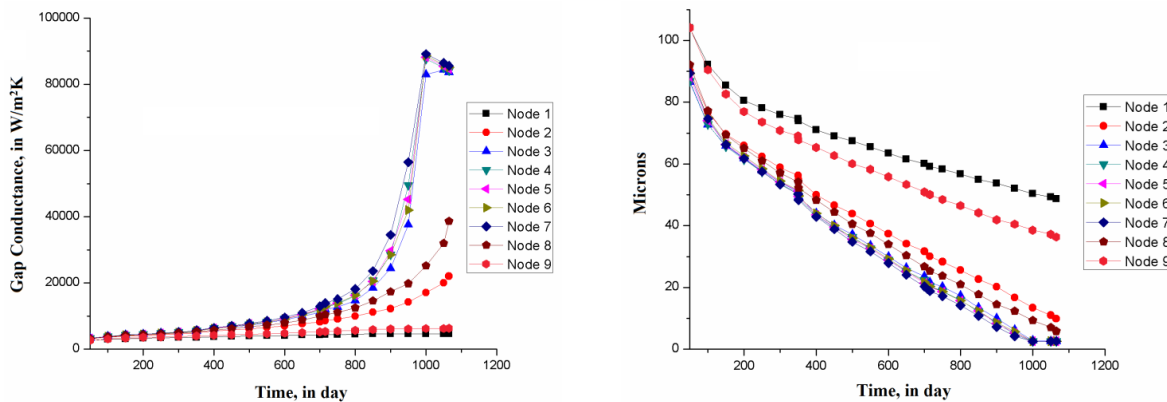


**Fig. 2.** Predicted gap conductance and gap thickness during 3 cycles.

The maxima of the average cladding outside surface ( $T_{co}$ ), oxide surface ( $T_{ox}$ ) and bulk coolant ( $T_b$ ) temperature are 609.1 K, 602.2 K and 582.6 K, respectively. The  $T_b$  value is close to average coolant temperature in core of 576.7 K [7]; this denotes that the cooling system always ensures the requirements for the operation.

### 3.2. Predicted deformation of fuel pellets

The results of deformation of fuel pellets were given in Fig. 3 (nominal value), including: Fuel stack axial extension, fuel swelling, fuel densification, fuel relocation and fuel thermal expansion.

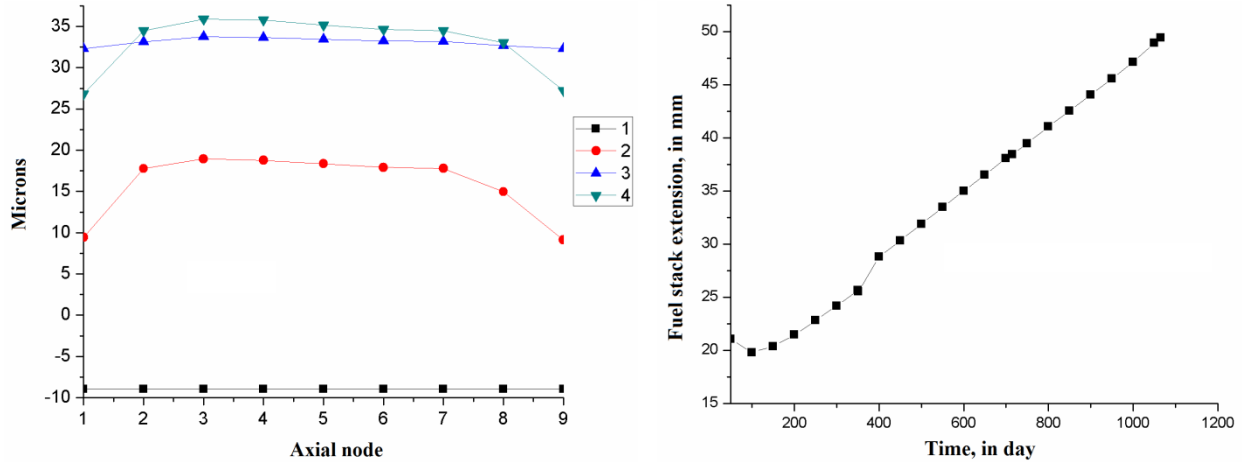


**Fig. 3.** Deformation of fuel pellets.

About 100 days of first cycle (burn-up about 5 to 10 GWd/tU), the re-sintering effect has the greatest effect on the deformation of the ceramic. The ceramic shrinkage was about 9  $\mu\text{m}$ , which reduces the length of the fuel column. Then, the effect of this phenomenon was gone.

The fuel pellets were deformed due to the influence of temperature, irradiation, and reactor operating conditions. The results show that during three cycles of operation, maximum fuel stack axial extension was 49.42 mm and the fuel clad gap was closure (see part 3.1). However, the rise of the fuel column and the disappearance of the capsule gap remain within the design limits of the AP-1000.

### 3.3. Predicted fission gas release and rod internal pressure

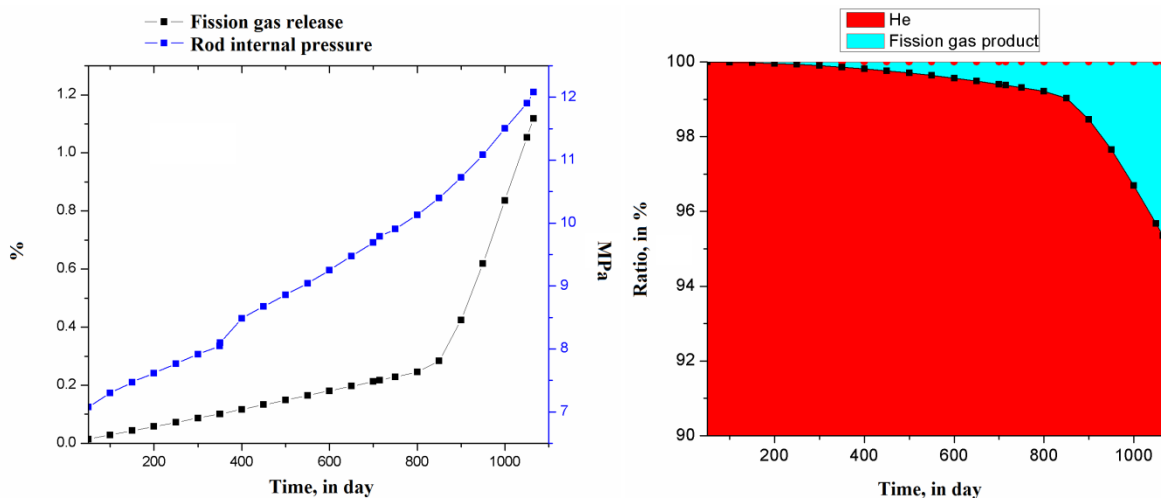


**Fig. 4.** Fission gas release and rod internal pressure.

Fission gas release (FGR) and rod internal pressure ( $P_i$ ) have a major impact on mechanical properties of fuel rod. Fission gas release can cause fuel swelling, pressure buildup

(xenon, krypton), pellet-cladding mechanical interaction, stress corrosion cracking, etc. So, the excessive fission gas release can cause the rod pressure to rise beyond system pressure and lead to fuel damage. Thus, rod pressure need to be limited by safety criteria and must be calculated for the design evaluation.

Maximum fission gas release of fuel rod (FGR) was 1.12 % at the end of 3<sup>rd</sup> cycle. Thus, almost all fission products were stored in pottery (in porous holes). Maximum rod internal pressure was 12.08 MPa during three cycles of operation and lower than the limit values [7]. The calculation results of FGR and internal pressure show the guarantee of design in order to protect the fuel against cladding lift-off. These results are lower than the limit values and show that they ensure to prevent the diametric gap between the fuel and the cladding from re-opening during steady state operation, which causes ballooning and affect the coolant flow or the local overheating of the cladding.

### 3.4. Predicted cladding oxidation and hydration

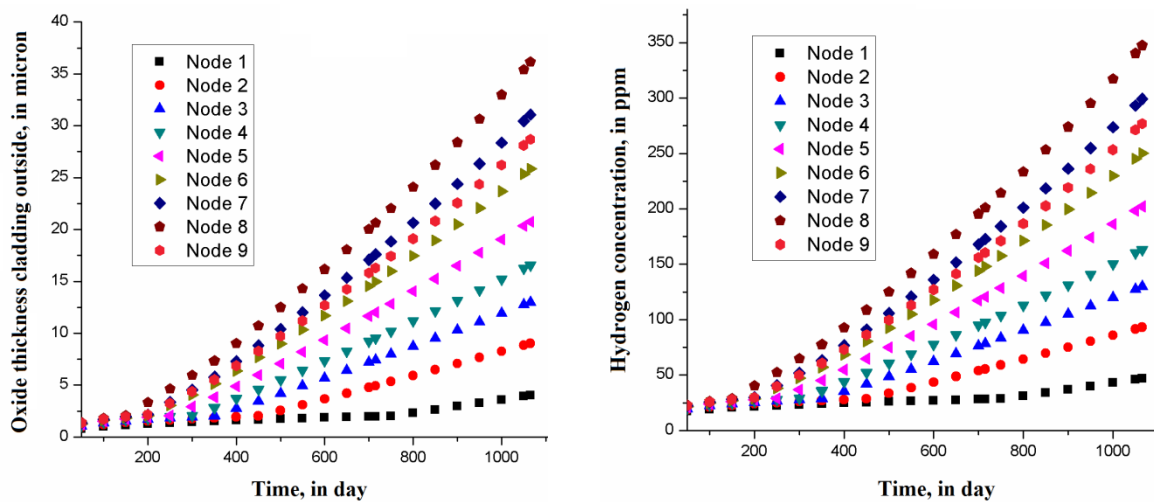


**Fig. 5.** Cladding oxide thickness and hydrogen concentration.

The results of oxide thickness and hydrogen concentration of cladding are given in Fig. 5 (nominal value). Oxidation and hydriding under normal operating conditions of reactor directly impact fuel performance, not only during normal operation, but during transients and accidents as well. Cladding corrosion reduces the effective thickness of the cladding, decreases the effective thermal conductivity of the cladding and thus increases the cladding and fuel temperatures and also reduces effective cladding-to-coolant heat transfer. Hydrogen absorption by the cladding and subsequent formation of hydrides may lead to cladding embrittlement. These phenomena are increasingly important at higher exposures. So, the analyses have to show ability to protect the fuel against any type of cladding corrosion induced failure.

The results of surface corrosion and cladding hydration calculation show that maximum oxide thickness was 36.13  $\mu\text{m}$  and maximum hydrogen concentration was 347.29 ppm during three cycles and lower than the limit values [7]. As such, the cladding rod was ensuring safety during the operation of the nuclear reactor.

## **CONCLUSION**

Thermal behavior of AP-1000 nuclear reactor fuel rod under steady state operating condition was predicted by using FRAPCON-4.0 simulation software. Predictive data show that the fuel centerline temperature reaches the maximum of 1404.4 K at 3 cycles and was lower than the limit value of the AP-1000 nuclear reactor fuel rod design; the maximum of average bulk coolant temperature was 582.6 K and close to the average coolant temperature in core. Gas temperature also predicted, plenum gas about 610 K and gas temperature in the gap about 630 K at the end of cycle 3. The calculation values by FRAPCON-4.0 code met acceptance criteria and suggested the fuel rod temperature image in nuclear reactor. The deformation of fuel pellets, fission gas release and rod internal pressure, cladding oxidation and hydration were predicted. The predicted values were lower than the limit values and fuel rod was ensuring safety during the operation of the nuclear reactor.

## **ACKNOWLEDGMENTS**

Authors would like to acknowledge the financial support from project, code DTCB.08/17/VCNXH, Vietnam Atomic Energy Institute; and FRAPCON and FRAPTRAN code support from Vietnam Atomic Energy Agency.

## **REFERENCES**

- [1] D. Olander, "Nuclear fuels – Present and future", J. Nucl. Mater, 389 (2009) 1–22.
- [2] Nuclear Fuel Cycle Information System, "A Directory of Nuclear Fuel Cycle Facilities", IAEA-TECDOC-1613 (2009)
- [3] KJ Geelhood, WG Luscher, PA Raynaud, IE Porter, "FRAPCON-4.0: A Computer Code for the Calculation of Steady-State, Thermal-Mechanical Behavior of Oxide Fuel Rods for High Burn-up", PNNL-19418, Vol. 1 Rev. 2, Pacific Northwest National Laboratory, Richland, Washington (2015).
- [4] KJ Geelhood and WG Luscher, "FRAPCON-4.0 Integral Assessment", PNNL-19418 Vol. 2 Rev. 2, Pacific Northwest National Laboratory, Richland, Washington (2015).
- [5] KJ Geelhood and WG Luscher, "Material Property Correlations: Comparisons between FRAPCON-4.0, FRAPTRAN-2.0, and MATPRO", PNNL-19418 Rev. 2, Pacific Northwest National Laboratory, Richland, Washington (2015).

- [6] N.T. Hung, L.B. Thuan, T.C. Thanh, H. Nhuan, D.V. Khoai, N.V. Tung, J.Y. Lee, J.R. Kumar, “Modeling the UO<sub>2</sub> ex-AUC pellet process and predicting the fuel rod temperature distribution under steady-state operating condition”, Journal of Nuclear Material, 504(2018) 191-197.
- [7] Westinghouse AP-1000 Design Control Document Rev. 19 – Tier 2: Material, Chapter 4; Reactor, 2011.
- [8] Final Safety Evaluation Report, Related to Certification of the AP-1000 Standard Plant Design, Volume 2 Supplement 2 Docket No. 52-006, NUREG-1793, United States Nuclear Regulatory Commission (2004).
- [9] I Arana, C Munoz-Reja and F Culbebras, “Post-Irradiation Examination of High Burnup Fuel Rods from Vandellos II”, Presented in Transactions of the Top Fuel 2012 Reactor Fuel Performance Conference, September 2-6, Manchester, UK, European Nuclear Society (2012).
- [10] Aaron M. Phillippe, Larry Ott, Kevin Clarno, Jim Banfield, “Analysis of the IFA-432, IFA-597 and IFA-597mox Fuel Performance Experiments by FRAPCON-3.4”, ORNL/TM-2012/195, Oak Ridge National Laboratory (2012).



# **DỰ ĐOÁN TRẠNG THÁI THANH NHIÊN LIỆU TRONG ĐIỀU KIỆN VẬN HÀNH ỔN ĐỊNH CỦA Lò PHẢN ỨNG HẠT NHÂN AP-1000 BẰNG PHẦN MỀM MÔ PHỎNG FRAPCON**

*Nguyễn Văn Tùng, Nguyễn Thanh Thủy, Cao Duy Minh, Nguyễn Trọng Hùng  
Viện Công nghệ xạ hiếm – 48 Láng Hạ, Đống Đa, Hà Nội  
Email: [tungnv.88@gmail.com](mailto:tungnv.88@gmail.com)*

Báo cáo này trình bày các kết quả về các dự đoán trạng thái của thanh nhiên liệu lò phản ứng hạt nhân AP-1000 trong điều kiện vận hành trạng thái ổn định bằng cách sử dụng phần mềm FRAPCON-4.0. Các dự đoán về phân bố nhiệt độ trong thanh nhiên liệu bao gồm nhiệt độ đường tâm nhiên liệu, nhiệt độ bề mặt viên nhiên liệu, nhiệt độ khí trong khoảng trống viên – vỏ, nhiệt độ bề mặt trong và bề mặt ngoài vỏ bọc thanh nhiên liệu, nhiệt độ lớp oxit bề mặt ngoài vỏ bọc thanh nhiên liệu và nhiệt độ lớp cặn bám trên bề mặt ngoài vỏ bọc thanh nhiên liệu; độ dẫn nhiệt và độ dày khoảng cách viên – vỏ. Các dữ liệu dự đoán cho thấy hình ảnh trạng thái nhiệt của thanh nhiên liệu trong lò phản ứng hạt nhân. Các dự đoán cũng bao gồm biến dạng của các viên nhiên liệu, sự phát thải khí phân hạch và áp suất bên trong của thanh nhiên liệu, sự oxi hóa và hydrua hóa lớp vỏ bọc thanh nhiên liệu.